**Figure 1.**

Scenario (a)

Base State 2035
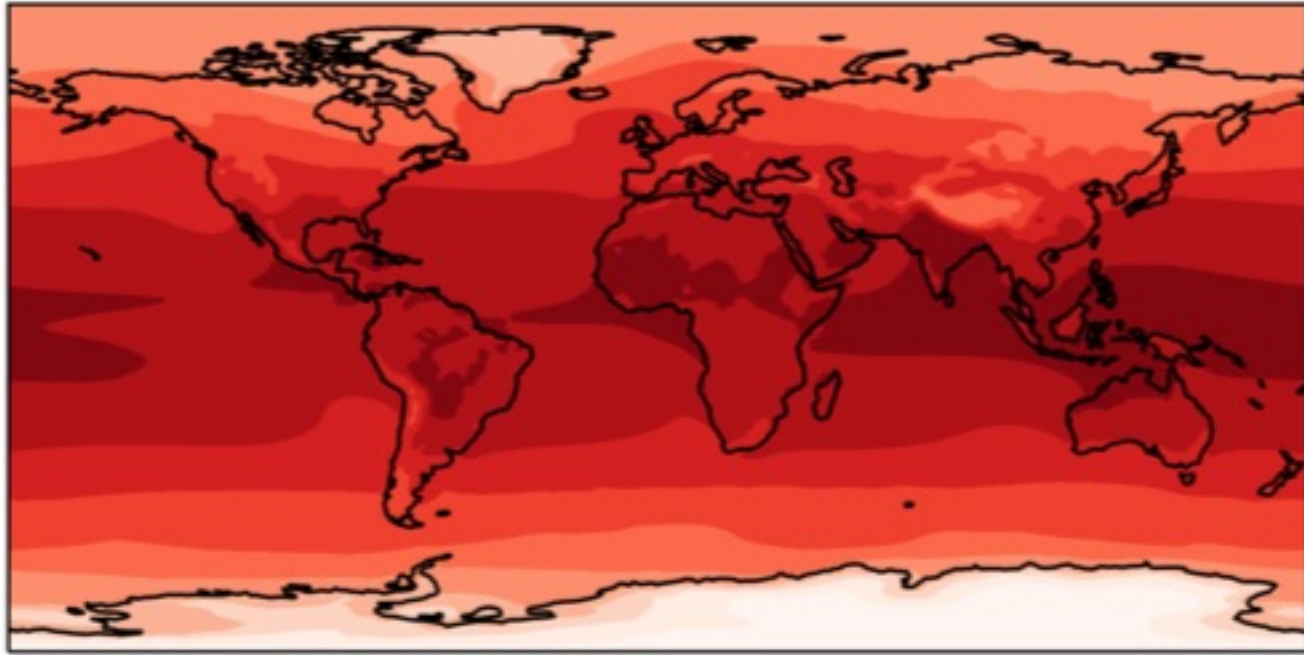
NAO −1.2 to −1.0
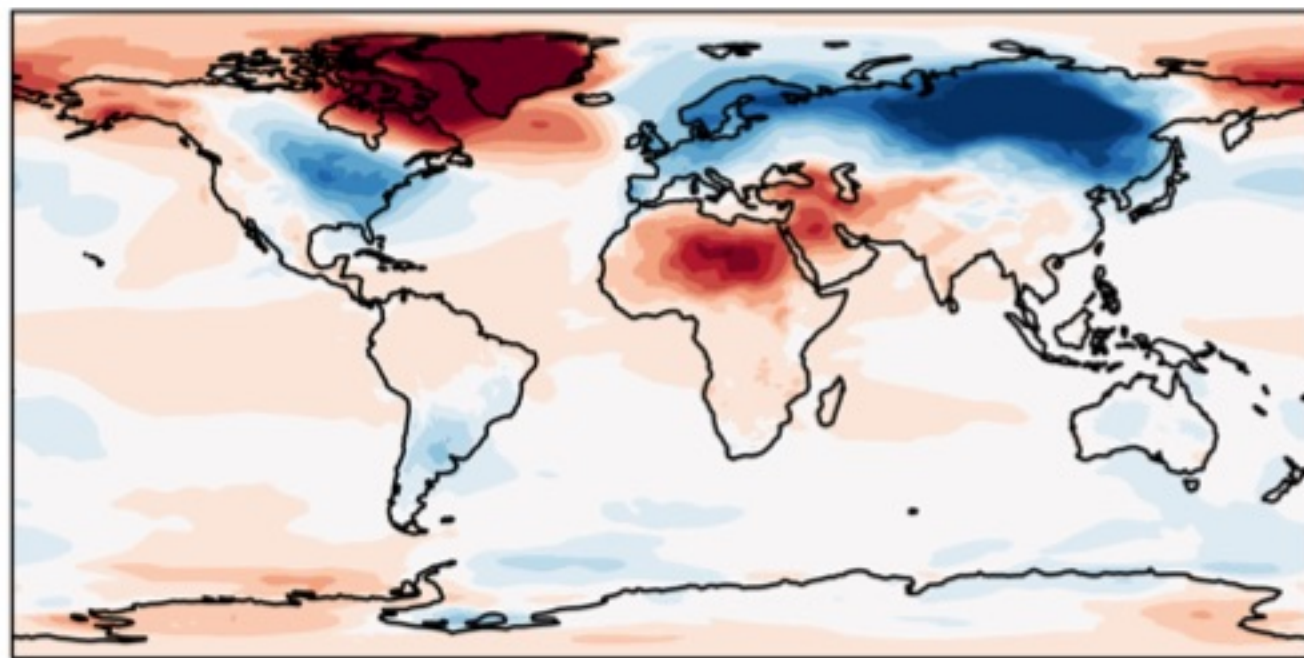
ENSO 1.0 to 1.2
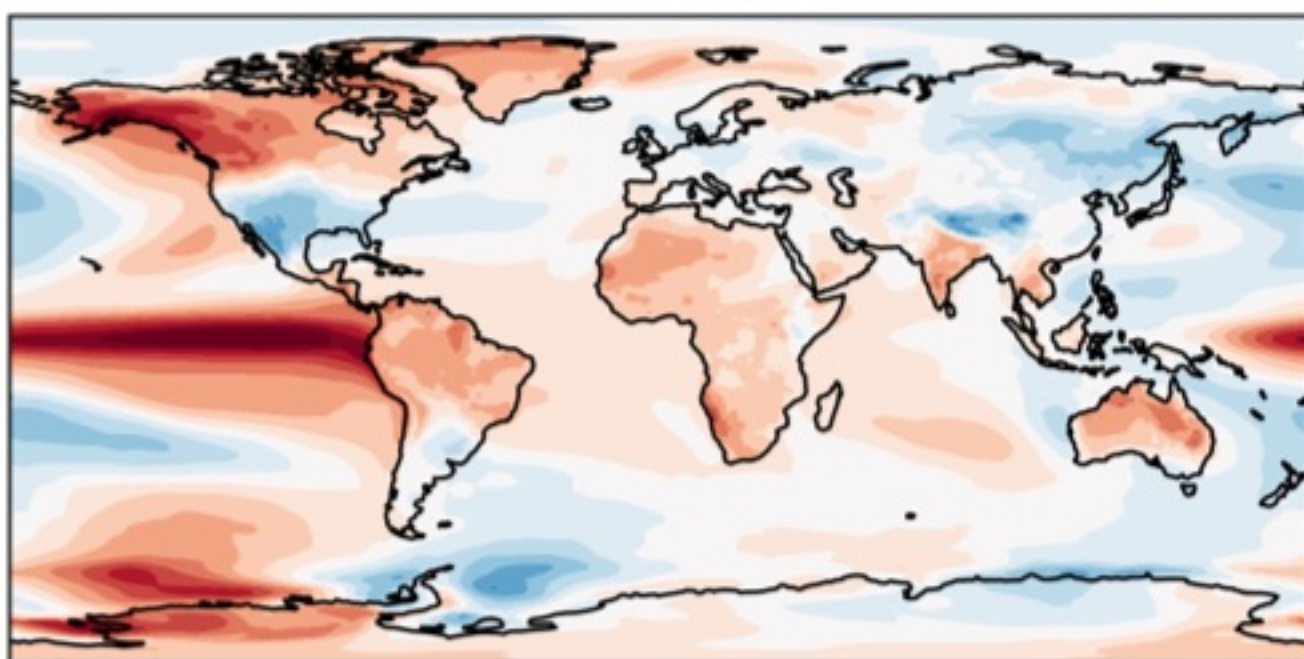
Base Injection = 0.43 Tg/year

New Injection = 0.71 Tg/year

Percent Change = 65.1%

Scenario (b)

Base State 2045
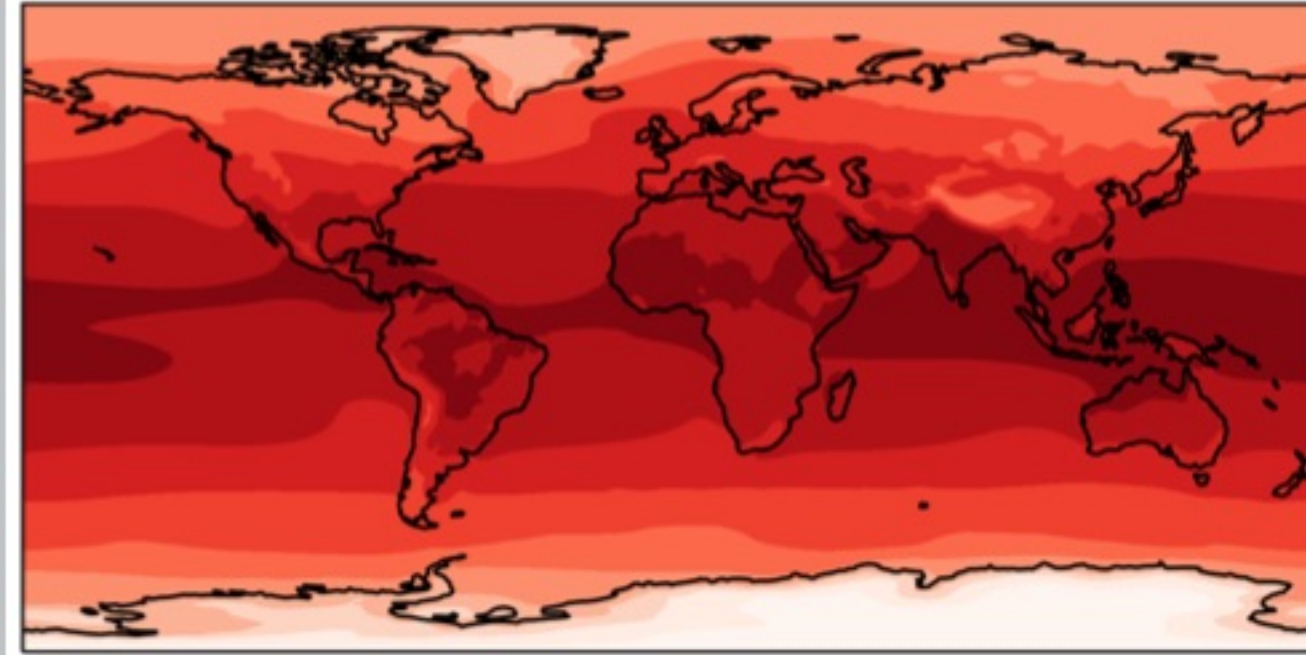
NAO −1.2 to −1.0
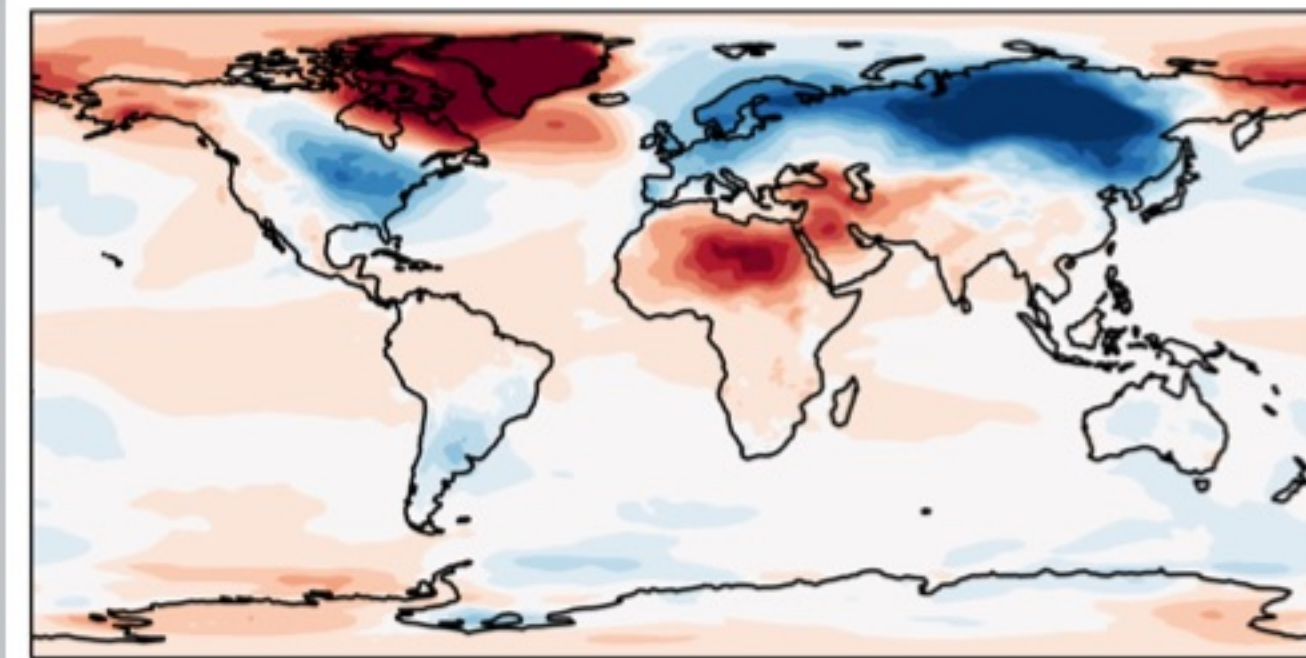
ENSO 1.0 to 1.2
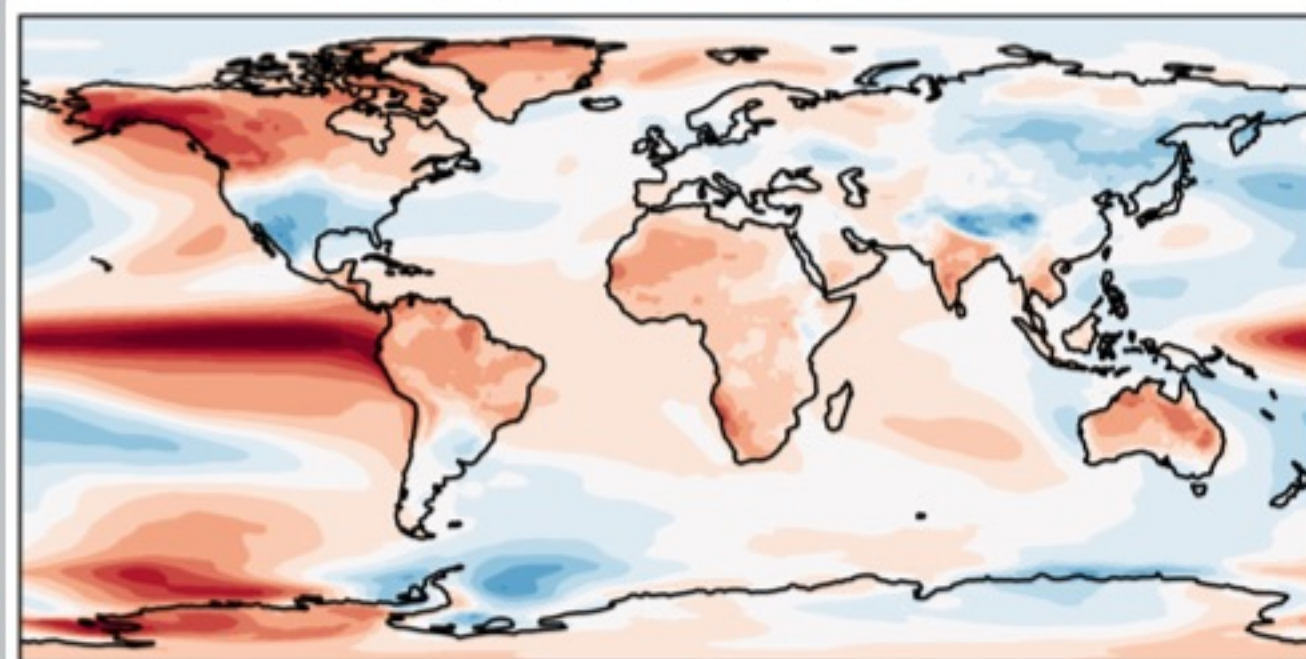
Base Injection = 1.44 Tg/year

New Injection = 1.56 Tg/year

Percent Change = 8.3%

Temperature (K)

310
301
292
283
274
266
257
248
239
230

Temperature Anomalies (K)

1.0
0.5
0.0
−0.5
−1.0

Figure 2.

Figure 3.

Percent Change
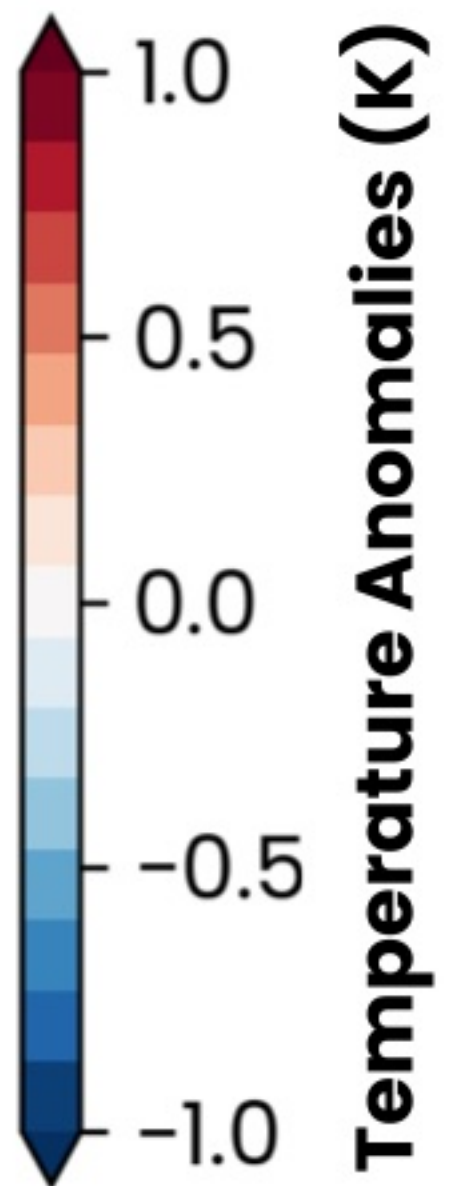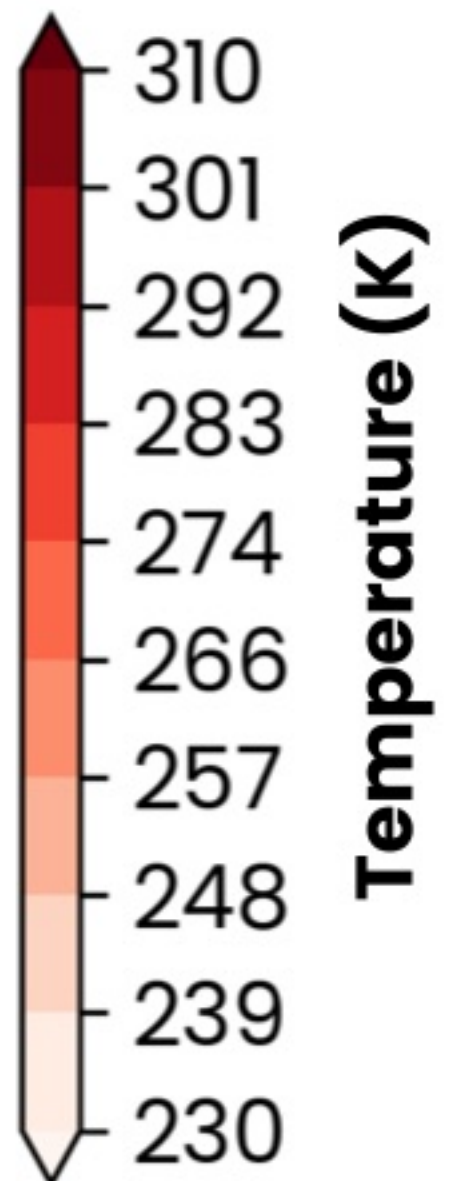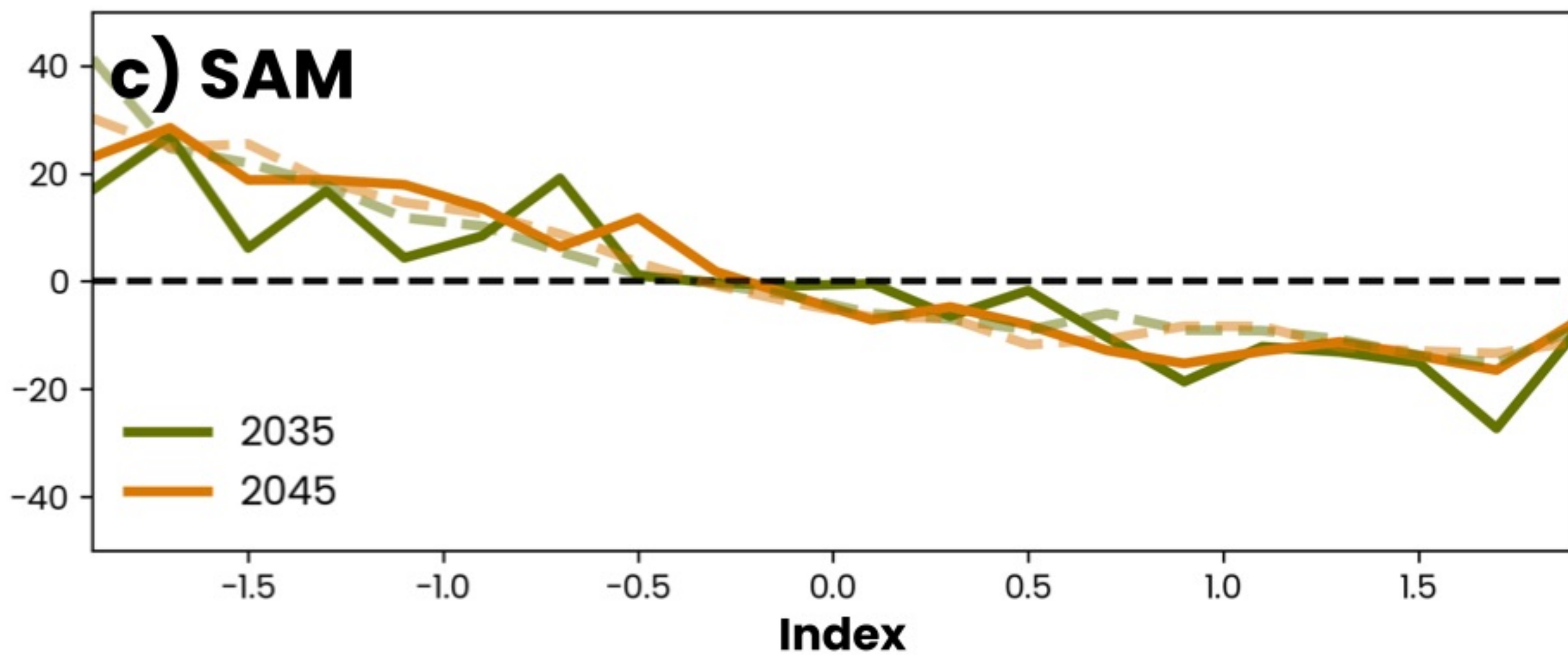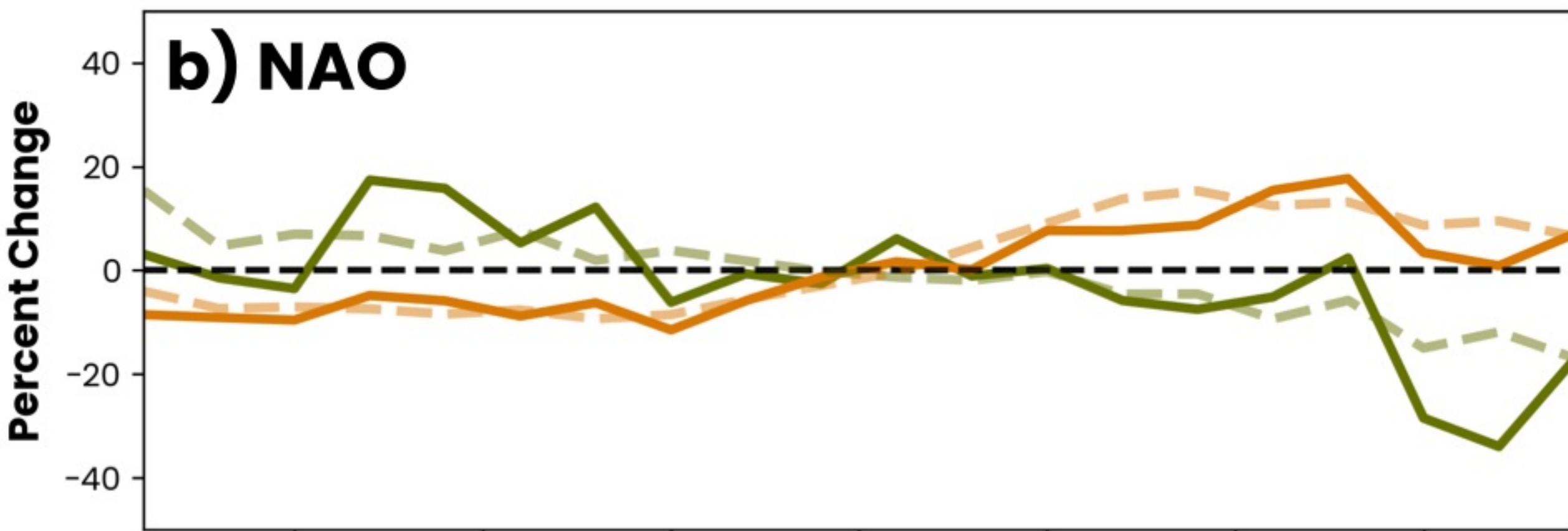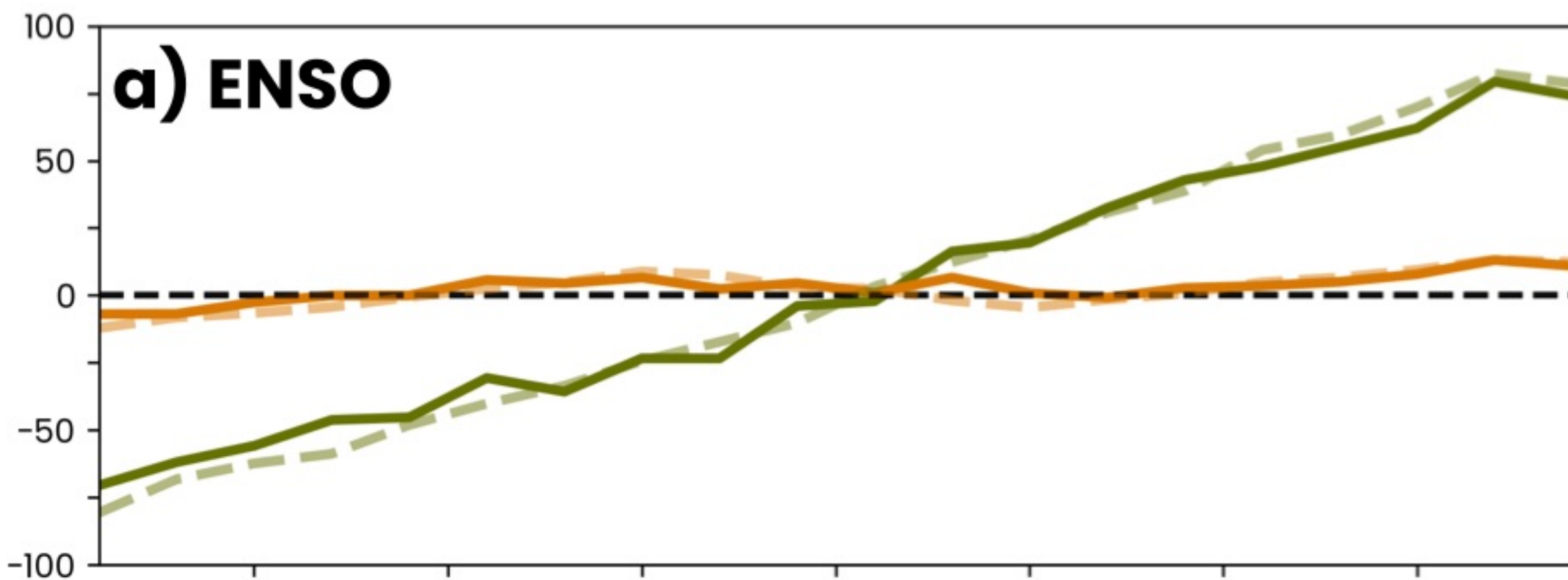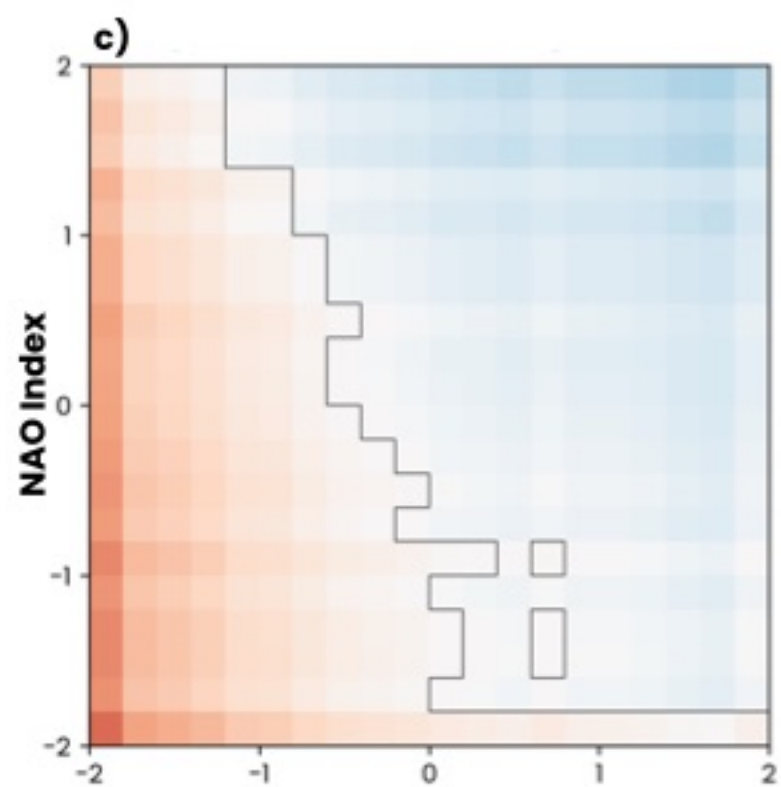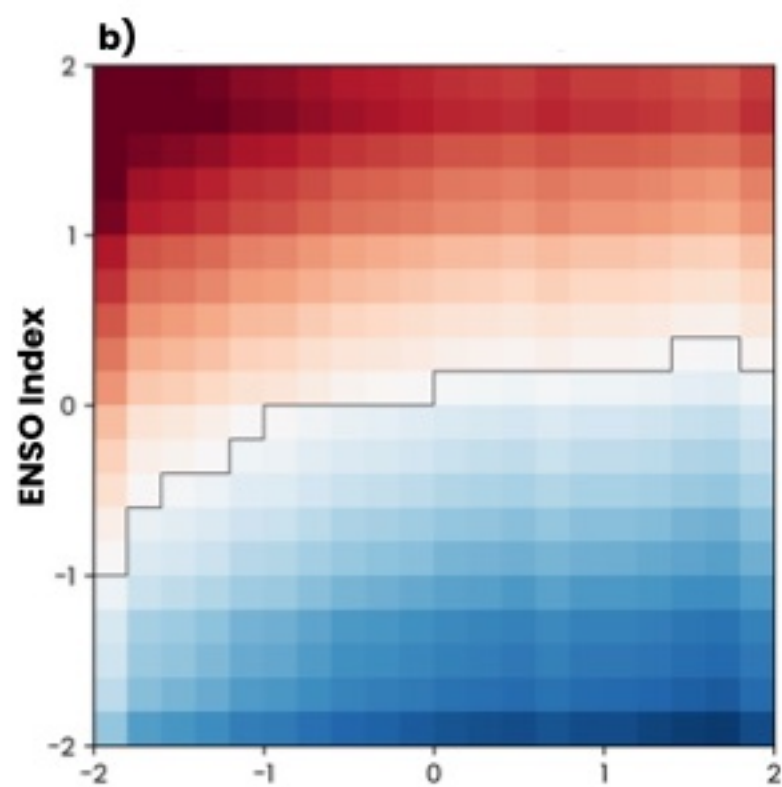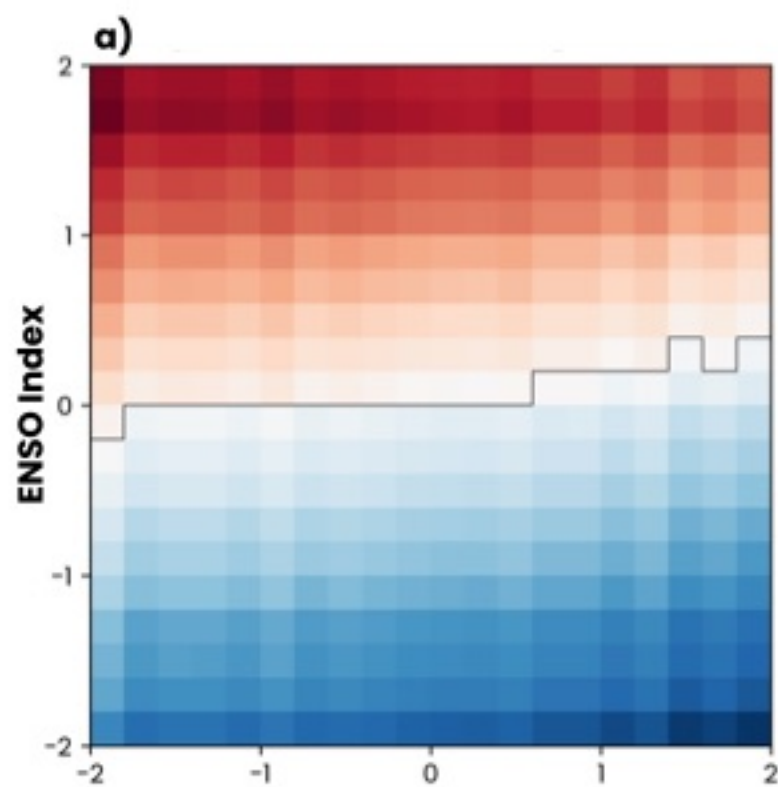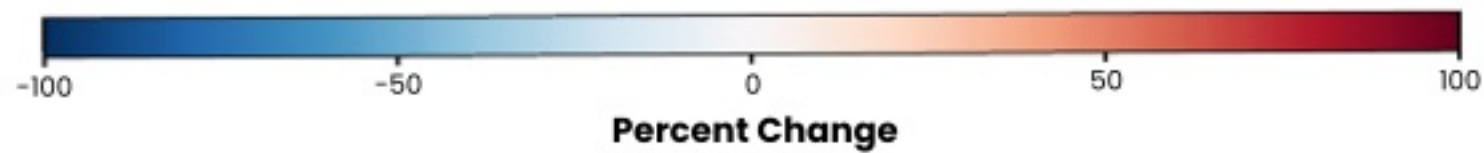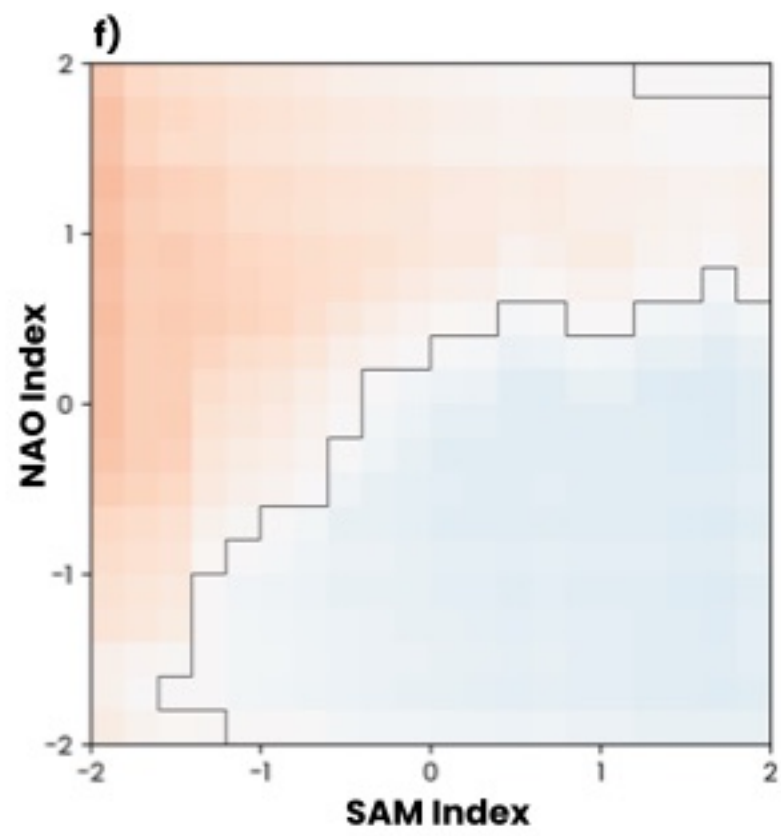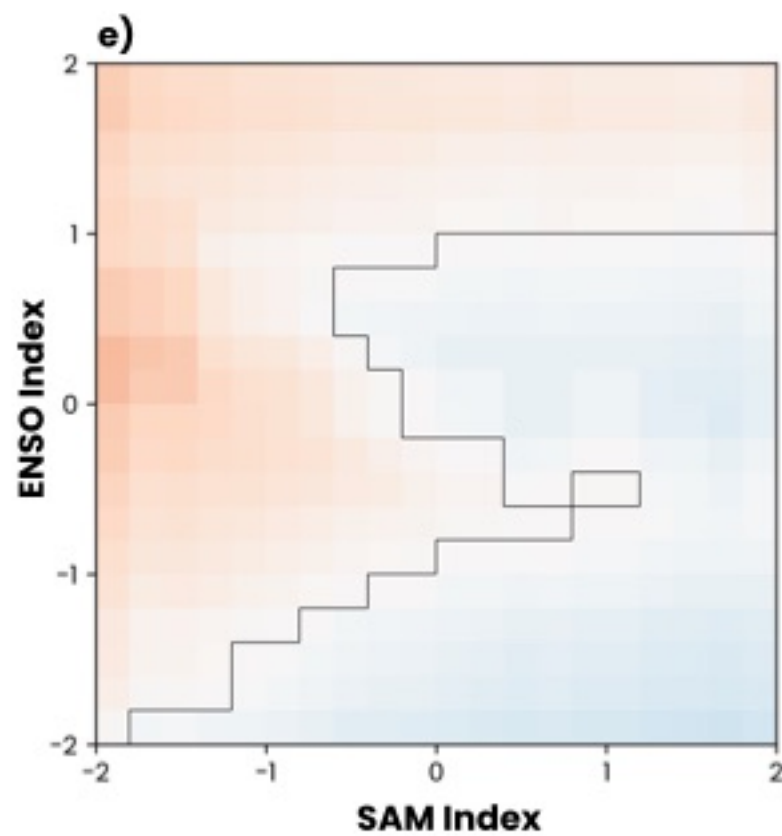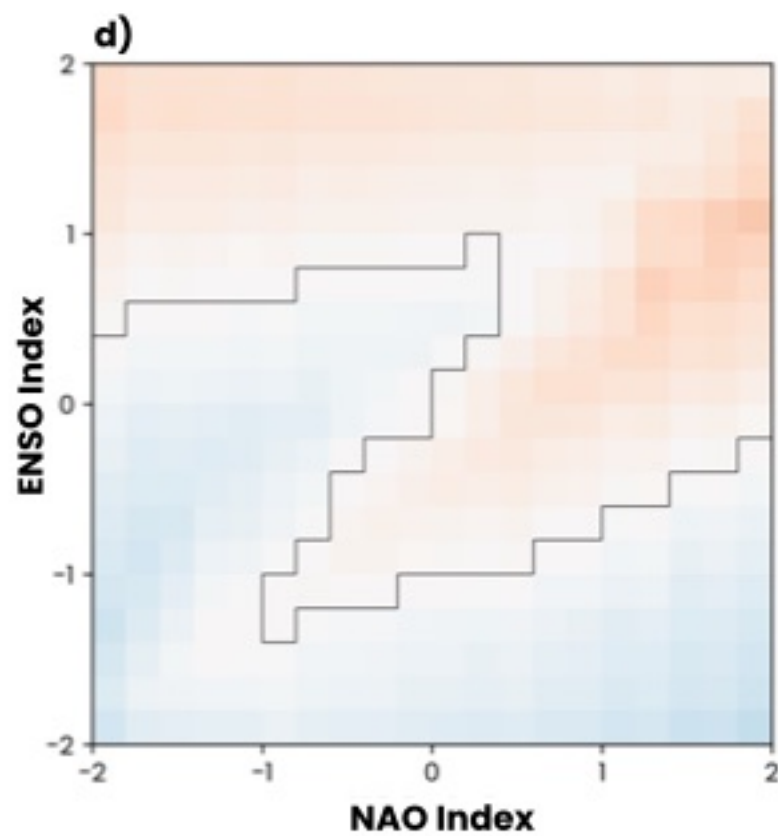
Figure 4.

a) Pinatubo eruption pattern

Temperature Anomaly (K)
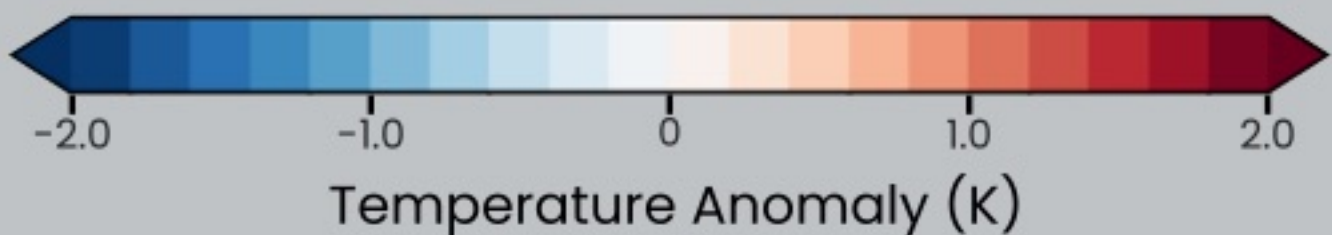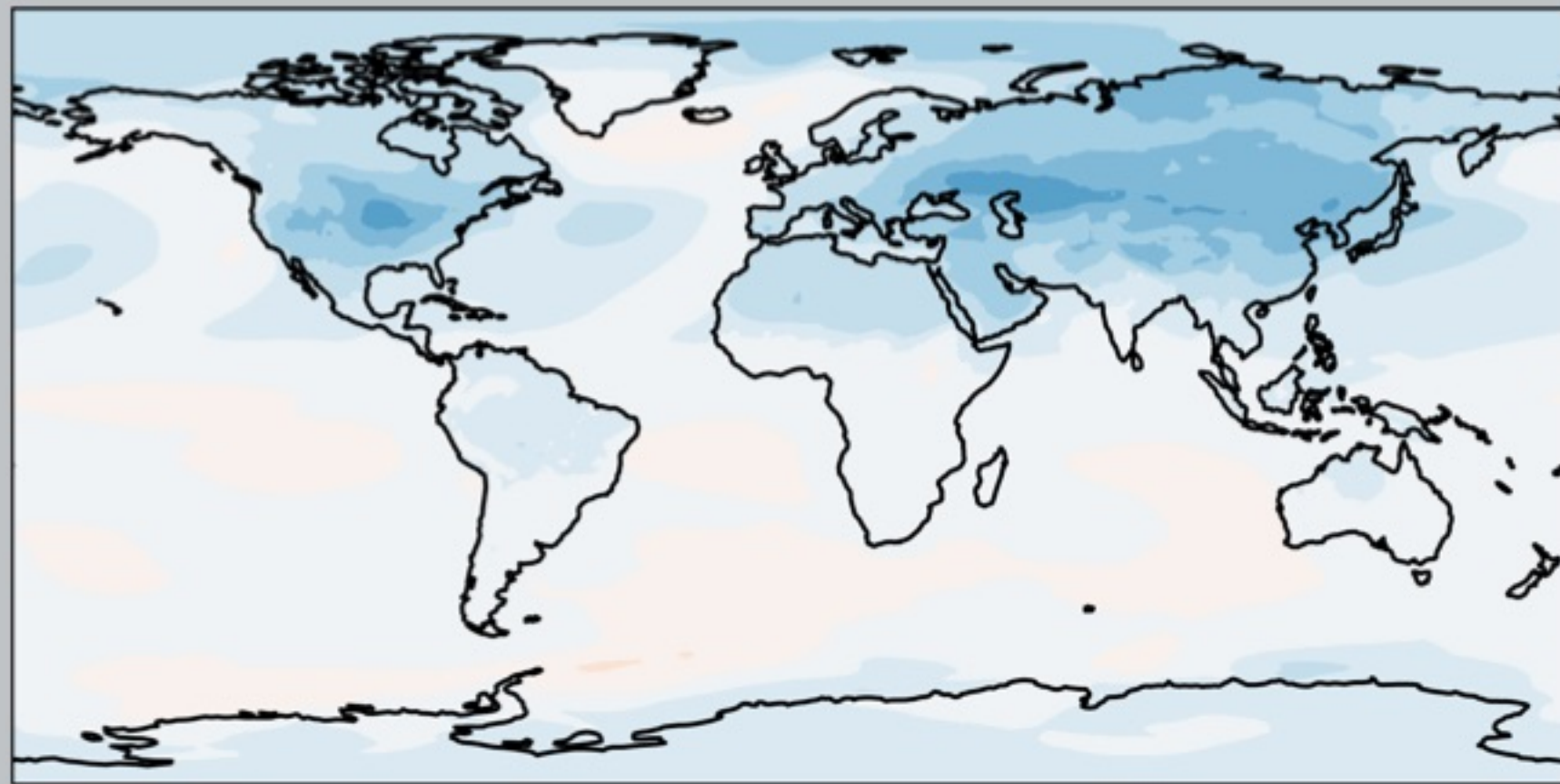
2035 Base Injection = 0.43 Tg/year
2035 New Injection = 0 Tg/year
Change = −0.43 Tg/year

2045 Base Injection = 1.44 Tg/year
2045 New Injection = .86 Tg/year
Change = −0.58 Tg/year

b) ENSO and Pinatubo

2035
2045
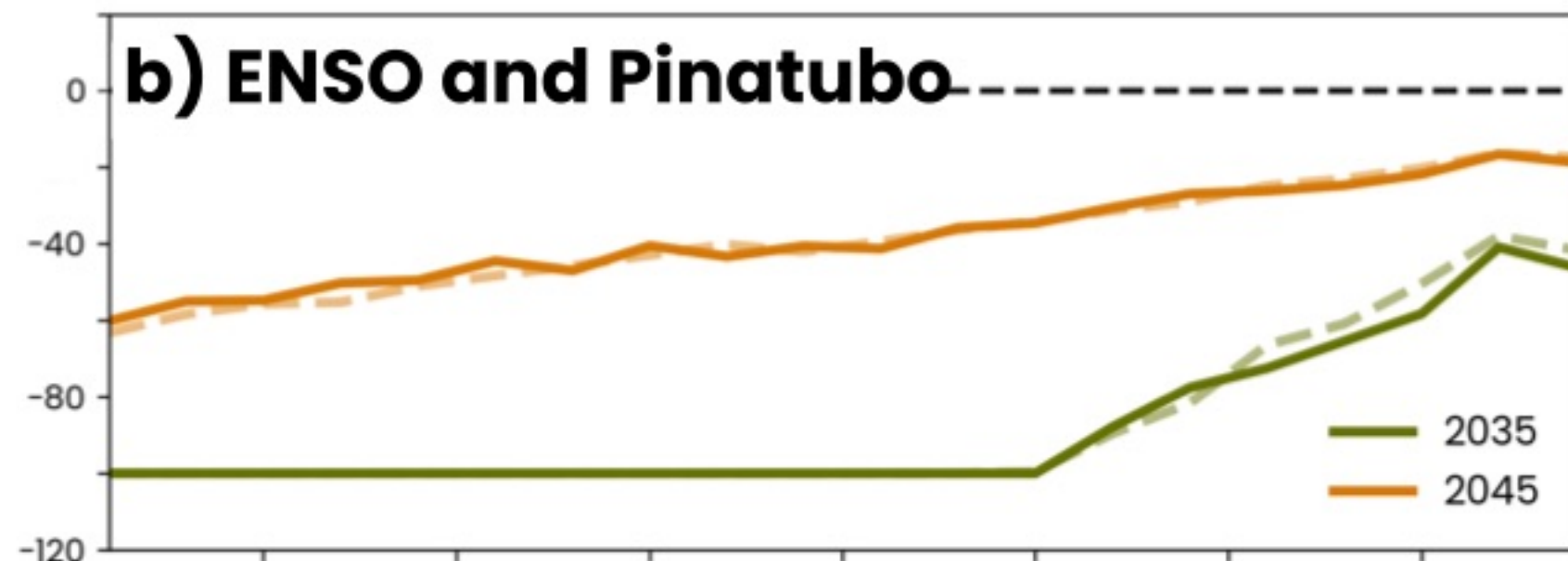
c) NAO and Pinatubo

d) SAM and Pinatubo

Percent Change

Index
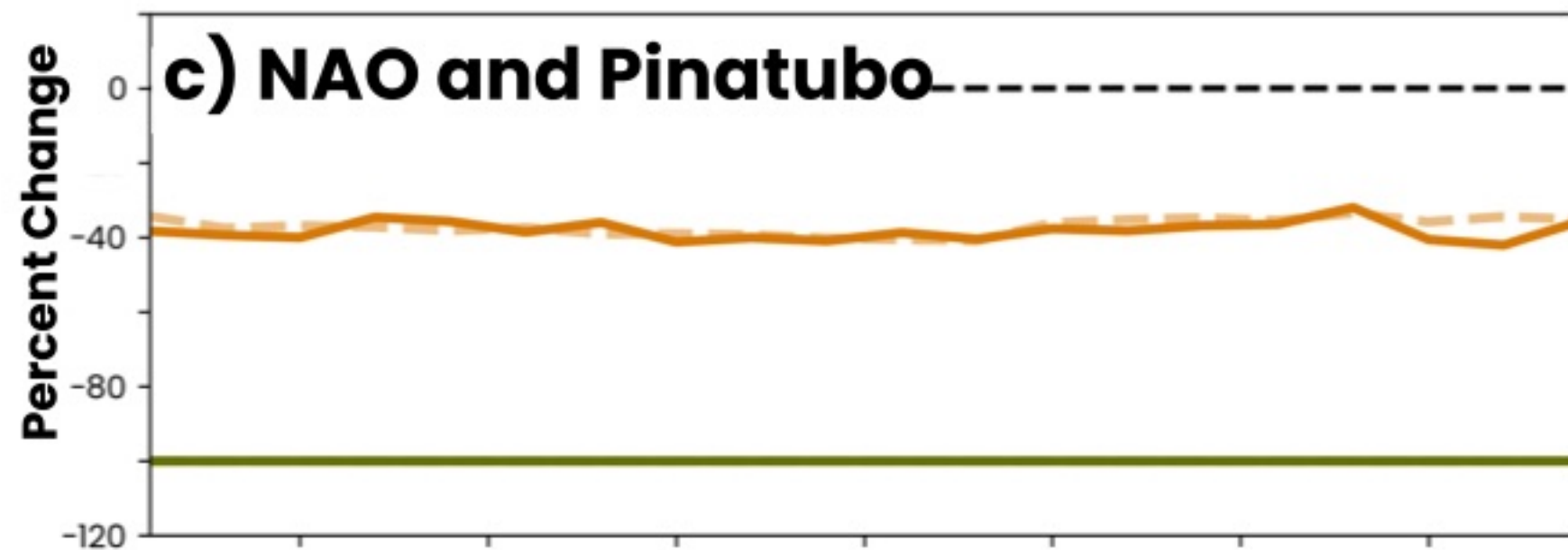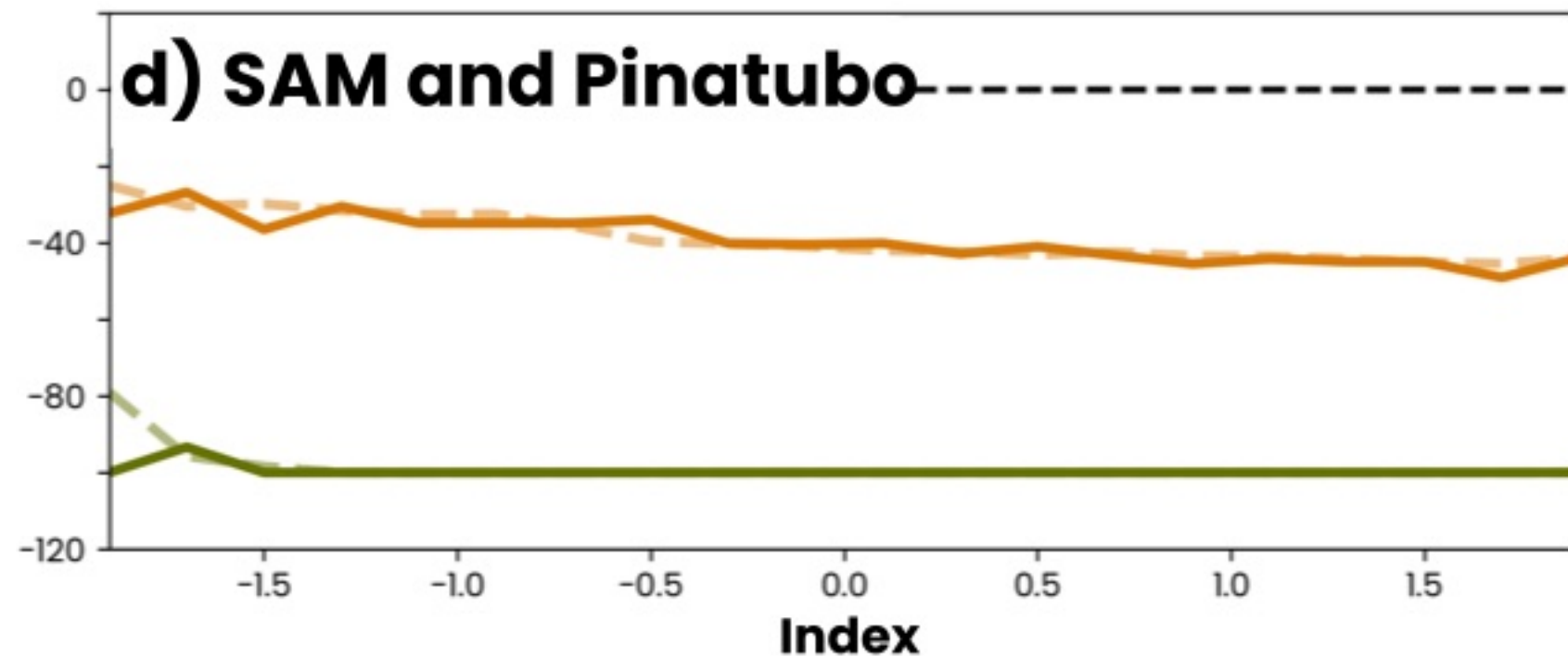
Quantifying the Impact of Internal Variability on the CESM2 Control Algorithm for Stratospheric Aerosol Injection

Charlotte Connolly[1], Emily Prewett[1], Elizabeth A. Barnes[1], James W. Hurrell[1]

[1]Department of Atmospheric Science, Colorado State University, Fort Collins, CO, USA

Key Points:

- We quantify how the ARISE-SAI controller responds to different patterns of internal variability.
- The impact from internal variability on the controller-determined injection is dependent on the background warming.
- This method provides a straight-forward way to cheaply quantify controller sensitivity to internal variability.

Corresponding author: Charlotte Connolly, `cconn@rams.colostate.edu`

Abstract

Earth system models are a powerful tool to simulate the response to hypothetical climate intervention strategies, such as stratospheric aerosol injection (SAI). Recent simulations of SAI implement tools from control theory, called "controllers", to determine the quantity of aerosol to inject into the stratosphere to reach or maintain specified global temperature targets, such as limiting global warming to 1.5°C above pre-industrial temperatures. This work explores how internal (unforced) climate variability can impact controller-determined injection amounts using the Assessing Responses and Impacts of Solar climate intervention on the Earth system with Stratospheric Aerosol Injection (ARISE-SAI) simulations. Since the ARISE-SAI controller determines injection amounts by comparing global annual-mean surface temperature to predetermined temperature targets, internal variability that impacts temperature can impact the total injection amount as well. Using an offline version of the ARISE-SAI controller and data from CESM2 earth system model simulations, we quantify how internal climate variability and volcanic eruptions impact injection amounts. While idealized, this approach allows for the investigation of a large variety of climate states without additional simulations and can be used to attribute controller sensitivities to specific modes of internal variability.

Plain Language Summary

Stratospheric aerosol injection (SAI) is a proposed climate intervention strategy that injects aerosols into the stratosphere to mitigate some climate change impacts. Several studies that have used climate models to investigate how the atmosphere may respond to SAI implement "controllers" to determine how much aerosol to inject and where in order to achieve certain climate targets. This work explores how changes to the controller input can impact the amount of aerosol injected by a controller. Here we focus on the controller from the Assessing Responses and Impacts of Solar climate intervention on the Earth system with Stratospheric Aerosol Injection (ARISE-SAI) simulations. This specific controller uses the annual-mean surface temperature to determine how much aerosol to inject. Therefore, internal variability that impacts temperature can impact the total injection amount as well. To quantify how patterns of internal variability impact how much aerosol is injected, we isolate the ARISE-SAI controller and pass a variety of temperature patterns into it. While this method ignores some interactions between the controller and the climate simulation, it is a quick way to quantify the controller's sensitivity to a large variety of temperature patterns without additional simulations.

1 Introduction

Current actions and plans by global nations to reduce greenhouse gas emissions may not be enough to keep global warming under 2°C (Liu & Raftery, 2021; Raftery et al., 2017). Climate intervention strategies have been proposed as a solution to reduce some of the negative consequences associated with climate warming (Crutzen, 2006; Cicerone, 2006; National Academies of Sciences, Engineering, and Medicine, 2021). Stratospheric aerosol injection is one such strategy where global temperature increases could be reduced by reflecting a small percentage of incoming solar radiation with sulfate aerosols or other substances in the stratosphere. The magnitude and pattern of cooling is determined by the amount and location of sulfur dioxide (SO_2) injected into the stratosphere which forms the sulfate aerosols (Tilmes et al., 2017).

Several modeling projects have been conducted to understand how the climate system may respond to additional SO_2 in the stratosphere (Rasch et al., 2008; Kravitz et al., 2013, 2015; Tilmes et al., 2018; Richter et al., 2022). Many of these simulations implement "feedback control", a method from control theory, to maintain the system at pre-established targets (MacMartin et al., 2014; Tilmes et al., 2018; Richter et al., 2022).

For example, the Assessing Responses and Impacts of Solar climate intervention on the Earth system with Stratospheric Aerosol Injection (ARISE-SAI) simulations use a proportional-integral control algorithm, also known as a controller, to determine how much SO_2 to inject into the stratosphere in order to maintain pre-established temperature targets (Richter et al., 2022; Kravitz et al., 2017).

When a controller is implemented in simulations to maintain specified characteristics of the climate, the controller and the simulated climate system will impact each other. By design, the simulated climate system responds to the amount and location of the SO_2 injection determined by the controller; however, the controller is also impacted by variability in the climate system. A handful of studies have begun to explore how the controller and the system impact each other. For example, MacMartin et al. (2014) show that the way in which the controller is tuned and the lag between the controller input and the response of the system can impact the internal variability of the climate system. Diao et al. (2023) use data from the ARISE-SAI simulations to show that ENSO accounts for 70% of the year-to-year variability in injection anomalies determined by the controller.

In this work, we pass temperature maps with different internal variability patterns into an offline version of the AIRSE-SAI controller to further explore and quantify how internal variability impacts SO_2 injection amounts. This controller keeps global mean surface temperature near 1.5°C while also maintaining temperature gradients so that atmospheric circulations are minimally impacted. The controller accomplishes this by comparing the global temperature (T0), the north-south temperature gradient (T1) and the Equator-to-pole temperature gradient (T2) to predetermined targets of 288.64, 0.8767, and -5.89 respectively (MacMartin et al., 2014; Kravitz et al., 2017). Deviations between the T0, T1, and T2 values calculated from model output and the individual predetermined targets are used by the controller to determine how much SO_2 to inject at four different locations (30°N, 15°N, 15°S, 30°S). Since the controller determines injection amounts based on deviations of T0, T1, and T2 from their respective targets, global and regional temperature patterns driven by internal climate variability can impact injection amounts.

2 Methods

The ARISE-SAI controller sensitivity to internal variability is quantified by creating controller inputs, for which the warming pattern and the patterns of internal variability are known, and passing them to the controller. The way in which the warming patterns and patterns of internal variability are calculated is provided in section 2.1. An offline version of the ARISE-SAI controller is used to explore a large range of climate states without having to run additional simulations, and details about the changes made to the ARISE-SAI controller are in section 2.2.

2.1 Controller Inputs

Every controller input map contains one forced component which describes the climate warming trend. The forced component, or *base state*, is defined as the smoothed annual-mean ensemble mean near surface temperature using years 2035 to 2070 from the 10 member ARISE-SAI control simulation (ARISE-SAI-CTRL; (Richter et al., 2022)). However, since 10 members are not enough to remove all internal variability (Deser et al., 2012), the ensemble mean is smoothed by fitting a 3rd order polynomial to the time series at each grid point. The smoothed data that results from fitting the polynomial is used as the base states.

Unforced components, or *internal variability patterns*, are defined as monthly temperature anomalies composited based on internal variability events. This work focuses on variability associated with the El-Niño Southern Oscillation (ENSO; (Trenberth, 1997)) phenomenon, the Southern Annular Mode (SAM; (Ho et al., 2012)), the North Atlantic

Oscillation (NAO; (Hurrell & Deser, 2010)), and the eruption of Mt. Pinatubo (Holasek et al., 1996). These modes of variability are selected because each produces strong temperature anomalies in different regions of the globe. ENSO influences temperature predominantly at low latitudes, the NAO predominantly influences temperature at the high latitudes of the Northern Hemisphere, the SAM predominantly influences temperature the high latitudes of the Southern Hemisphere, and a Pinatuno-like volcanic eruption predominantly influences temperatures globally. Internal variability patterns of interest are added onto a base state to quantify their impacts on total injection amounts.

The climate indices used to composite temperature anomalies associated with ENSO, NAO, and SAM events are calculated using, sea surface temperature, and sea level pressure. Methods used to calculate each climate index are as follows:

1. ENSO index is defined by the ENSO 3.4 index (Trenberth, 1997) based on the five month average sea surface temperature within the 5°N-5°S, 120-170°W region.
2. The NAO index is defined by the principal component time series of the leading empirical orthogonal function of surface pressure anomalies within 20-80°N, 90°W-40°E (Hurrell & Deser, 2010).
3. The SAM index is calculated as the principal component of the leading empirical orthogonal function of sea level pressure over the region 20-90°S (Ho et al., 2012).

Anomalies used in the internal variability composites are calculated by subtracting the smoothed ensemble mean from each ensemble member and removing the seasonal cycle. Monthly temperature anomalies are used instead of annual to increase the amount of the data that goes into each composite. To support the robustness of the results, anomalies from years 2035-2070 from the 100 member CESM2 Large Ensemble historical simulation (CESM2-LE; (Rodgers et al., 2021)) are also used.

Despite ARISE-SAI using a moderate emissions scenario and CESM2-LE utalizing a moderate to high emissions scenario, our results are not impacted because the ensemble means are removed when calculating anomalies. The temperature anomaly pattern associated with the Mt. Pinatubo eruption is defined as the average temperature anomaly two years following the eruption (June 1991 - June 1993). Using the 100 member CESM2-LE. The climate warming trend is estimated by fitting a line at every grid point to the ensemble mean surface temperature anomalies time series 10 years prior to the eruption (May 1981 - May 1991). This line is extrapolated to June 1993, two years following the eruption, and then subtracted from the ensemble mean. Assuming the internal variability is removed by calculating the ensemble mean of 100 members and that the linear fit represents a short term continued warming trend, subtracting the linear fit from the ensemble mean estimates the temperature anomalies associated with the eruption of Mt. Pinatubo.

2.2 Changes to the Controller

The ARISE-SAI controller is a proportional-integral control algorithm, or PI controller (Åström & Murray, 2021). With a PI controller, the proportional term accounts for the current error between model output and the predetermined targets and the integral term accounts for any persistent errors in time. Constants, called gains, are tuned to determine how much of each component is needed to maintain the system at the user-specified targets (Jarvis & Leedal, 2012; MacMartin et al., 2014; Åström & Murray, 2021). The active controller in the ARISE-SAI simulations has a ramp up time of five years, which reduces shock to the system, and considers errors from previous years in the calculation via the integral portion of the controller. For more details about the complete ARISE-SAI simulations and its active controller, please refer to Richter et al. (2022) and Kravitz et al. (2017) and the sources within. This work utilizes an offline version of the ARISE-SAI controller where the gain values are kept the same (i.e. no addition tuning)

but the controller is not connected to an active simulation. A couple of additional changes are made to the offline ARISE-SAI controller for this work. First, the ramp up period is reduced from five years to one year because this work focuses on how internal variability impacts the total injection and doesn't need to worry about shocking the system. Second, the offline controller only receives one input at a time, therefore the controller does not have errors from previous years to use when calculating an injection amount for the current input. These changes ensure that when a temperature pattern is fed through the controller, the injection amount is determined by a single temperature pattern and not an evolving state.

3 Results

In this study, we focus on base states from year 2035 and year 2045 from the ARISE-SAI-CTRL. This replicates when SAI starts in the ARISE-SAI simulations and when SAI starts in the delayed intervention simulations (MacMartin et al., 2022). The delayed start simulations reduce temperature to the same ARISE-SAI targets and are designed to inform the impacts associated with delaying a decisions about SAI for 10 years. The total injection when only the base states are passed into the controller quantifies the total injection in response to the climate warming signal. For the base states of 2035 and 2045, the injections are 0.43 Tg/year and 1.44 Tg/year, respectively. Patterns of internal variability are then added onto these base states to create new controller inputs that, when passed into the controller, quantify the impact of internal variability on the total injection amounts.

Consider the three patterns shown in Scenario (a) in Figure 1: the base state from 2035, the temperature anomaly pattern associated with an ENSO index between 1.0 and 1.2, and the temperature anomaly pattern associated with NAO index between -1.2 and -1.0. When these three patterns are added together and then passed into the controller, the controller injects 0.71 Tg/year of SO_2 into the stratosphere. Adding the same internal variability patterns onto the base state 2045 (Scenario 2), the total injection increases to 1.56 Tg/year. The patterns of internal variability shown in Figure 1 are responsible for increasing the total injection by 0.28 Tg/year in 2035 and by 0.12 Tg/year in 2045. These increases are similar in magnitude, but in relation to the base injection, the impact from internal variability decreases from 2035 to 2045 by a factor of eight: 65.1% compared to 8.3%. This shows that while identical internal variability patterns added to 2035 and 2045 will always cause the T0, T1, and T2 values to deviate from their individual target values by the same amount, the amount of SO_2 injected in response to internal variability in 2035 is not equal to the amount of SO_2 injected in response to the same internal variability in 2045.

Since the impacts from internal variability on the controller-determined total injection depends on the base state, the ENSO, NAO, and SAM impacts on the total injection amounts are quantified as percent change using the 2035 and 2045 base states in Figure 2 (Figure 2 but for total change is in Supporting Information S1). Warm ENSO events increase the amount of SO_2 injected and cold ENSO events decrease the amount SO_2 injected (Figure 2a). This is not surprising considering that positive ENSO events are shown to increase the global average temperature, while negative events do the opposite (Angell, 1990). The stronger the ENSO event, the greater the impact on the total injection, although, the impact of ENSO anomalies on the controller decreases substantially from year 2035 to year 2045. This is because as the climate warming signal increases, the ENSO internal variability pattern is a smaller percentage of the input and so it plays a smaller role in the total injection amount.

The NAO has a smaller impact on the total injection in 2035 when compared to ENSO and its impact switches signs from 2035 to 2045. The SAM also has a smaller impact on the total injection then ENSO but its impact doesn't change from 2035 to 2045.
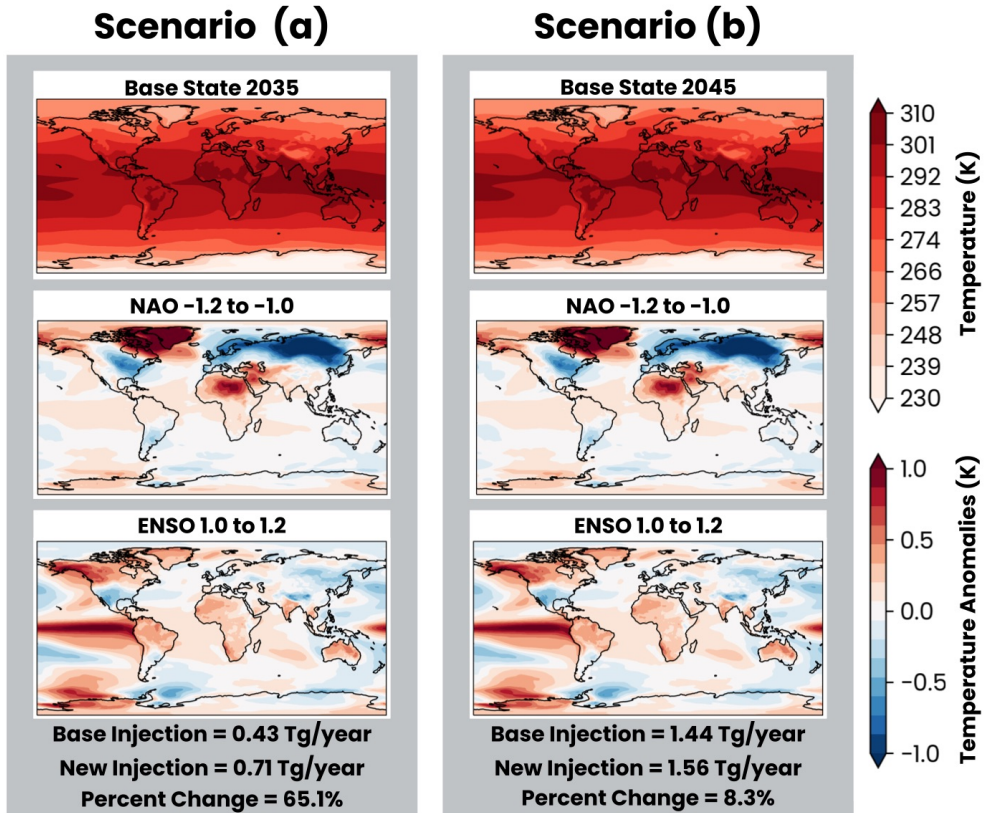
Figure 1. Schematic showing patterns that make up two different controller inputs. The base injection is the amount injected given only the base state while the new injection is the injection amount when all components are summed. Percent change shows how much internal variability changes the total injection as a function of the base state.
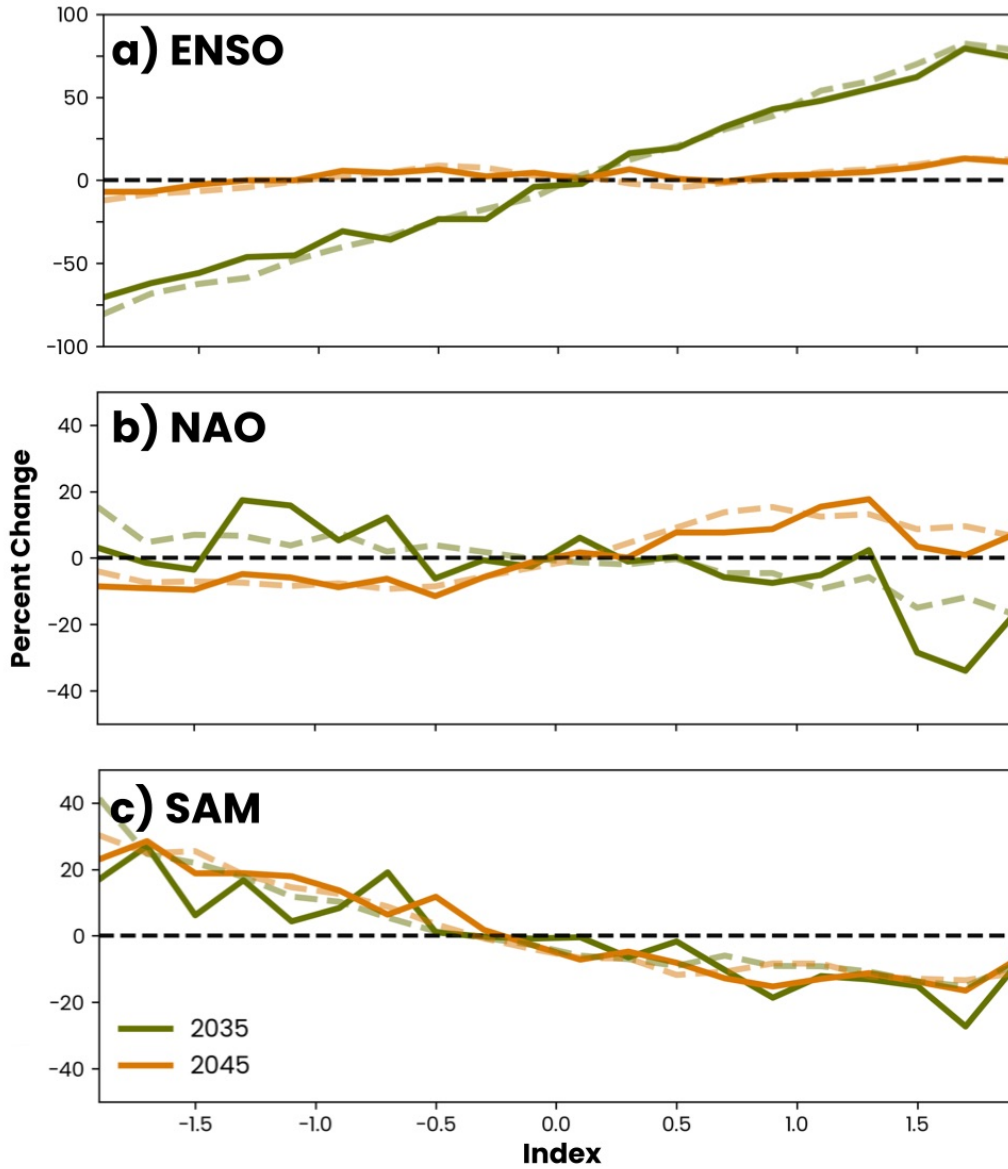
Figure 2. Percent change in total SO_2 injection as a function of (a) ENSO, (b) NAO, and (c) SAM events. Solid lines use data from ARISE-SAI-CTRL and dashed lines use data from CESM2-LE. Green lines use year 2035 base state and orange lines use year 2045 base state. Black dashed line marks zero percent change.
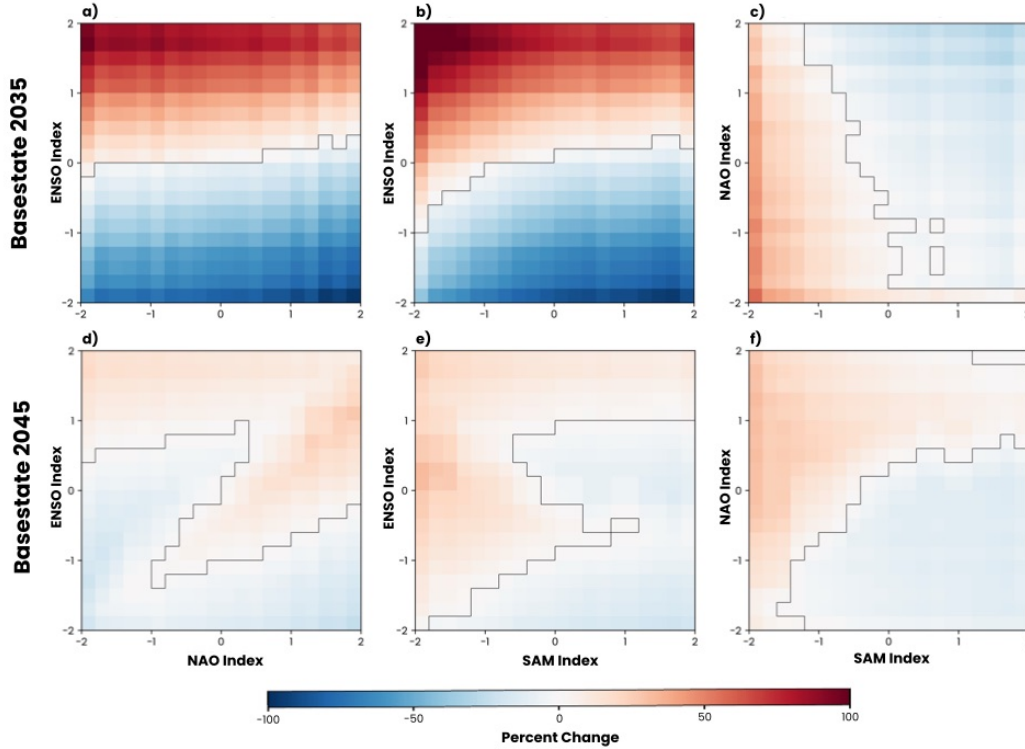
Figure 3. Percent change in total SO$_2$ injection as a function of two internal variability indices using composites from the CESM2-LE. Top row uses the year 2035 base state and bottom row uses the year 2045 base state. Black line in each panel separates positive percent change (red shading) from negative percent change (blue shading).

Similar SAM and NAO impacts exist in both the ARISE-SAI-CTRL and CESM2-LE data and are therefore likely not a result of noise in the composites, but an impact of the internal variability itself. In Figure 2, the base state pattern is the only difference between the green and orange lines in each panel, further demonstrating how the same internal variability pattern can have a different impact depending on the background state.

Taking our analysis one step further, Figure 3 shows how injection amount changes as a function of the combination of two climate indices with the top row depicting the base state from year 2035 and the bottom row year 2045. Given that the controller responds similarly whether anomalies are calculated from ARISE-SAI-CTRL or CESM2-LE data, Figure 3 shows results only using CESM2-LE anomalies. Results using ARISE-SAI-CTRL are in Supporting Information S2.

Adding two internal variability patterns onto a base state can increase or decrease the total injection more than the individual internal variability patterns (Fig. 3). When using the 2035 base state, the largest impacts typically occur when the internal variability events are the strongest, as shown by the largest magnitudes of percent change found in the corners of the top row panels in Figure 3. For a base state year of 2045 (bottom row), we find that the largest magnitude changes no longer necessarily occur when the internal variability events are strongest. For instance, when the NAO is positive, the strongest impact to the total injection occurs when the ENSO index is near one rather than two (Fig. 3d). When looking at the T0, T1, and T2 errors for the individual temperature patterns in Figure 3 (not shown), the sign of the T1 error relative to the T1 target (.8767)
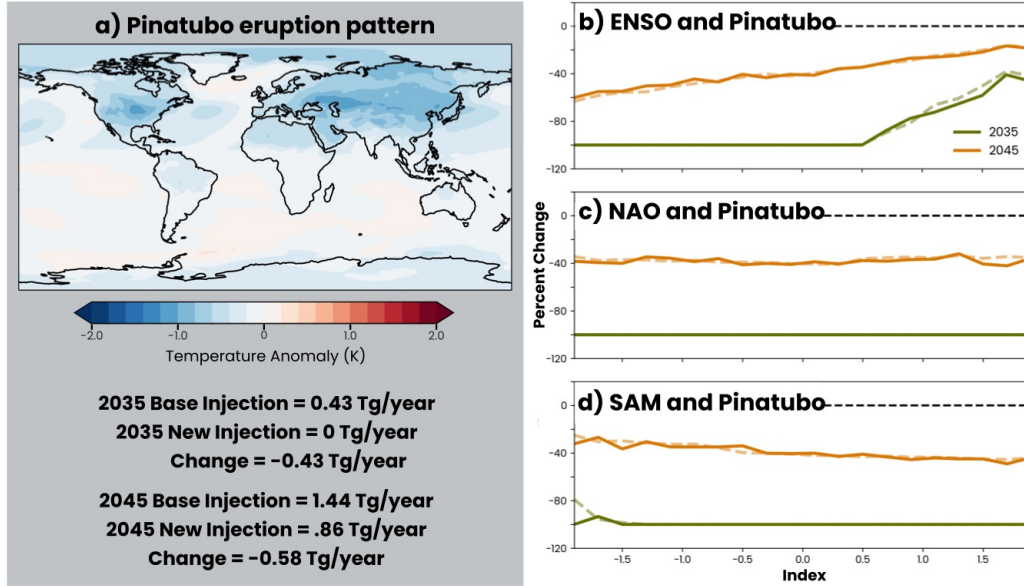
Figure 4. Mt. Pinatubo's impact on the total injection where (a) are the temperature anomalies associated with the Mt. Pinatubo eruption (volcano component of controller input). The new injection is the total SO_2 injected given the base state and the volcano component. Percent change shows as a function of the base state, how much the Mt. Pinatubo eruption changes the total injection. Panels (b), (c), and (d) are similar to Figure 2 but also include the volcano component in the controller input.

changes sign from negative in 2035 to positive in 2045 while the sign of T0 and T2 errors stay the same. The T1 value describes the north-south temperature gradient where a positive T1 value means the Northern Hemisphere is warmer than the Southern Hemisphere and so the sign change in T1 errors is likely in response to the uneven hemispheric warming that occurs in response to climate change.

We now explore the controller sensitivity to a volcanic eruption represented by the temperature anomaly pattern associated with the 1991 Mt. Pinatubo eruption (Figure 4a). Introducing the volcanic eruption temperature pattern to the 2035 and 2045 base states decreases the amount of SO_2 the ARISE-SAI controller injects. When the volcanic pattern is added to the 2035 base state alone, the controller injects nothing and when added to the 2045 base state, the injection decreases by about 40%. The Mt. Pinatubo eruption injected approximately 10 Tg of SO_2 into the stratosphere (Wilson et al., 1993; Bluth et al., 1992) and previous work estimates that it cooled the Earth's surface by 0.5°C (Parker et al., 1996). Therefore, a volcanic eruption the size of the Mt Pinatubo eruption would reduce the errors in T_0 and thus decrease the total injection determined by the controller. In 2035, the global cooling is response to a Pinatubo-like eruption is enough to negate all experienced global-mean warming (at least from the controller's perspective), removing the need to inject any SO_2. The amount of SO_2 naturally injected by Mt Pinatubo is not enough to combat the amount of warming experienced in 2045.

Including an internal variability pattern in addition to the Mt. Pinatubo eruption pattern allows for the quantification of how much a Pinatubo-like eruption in combination with internal variability impacts the controller-determined SO_2 injection (Figure 4b, c, and d). In 2035, when a Pinatubu-like eruption removes the need to inject SO_2, only an ENSO event stronger than 0.5 forces the controller to inject. Warming associated with

a positive ENSO greater than 0.5 is enough to cause the ARISE-SAI controller to inject despite the volcanic eruption. In 2045, a Pinatubo-like eruption decreases the total injection by about 40% as shown by the orange lines in panels Figure 4b, c, and d. Based on results in Figure 4b, c, and d, a volcanic eruption decreases the in injection amount by 0.43 Tg/year in 2045 and by 0.58 Tg/year in 2045.

4 Discussion

By design, controllers respond to variability of a system and therefore work well in systems with uncertainty. However, a controller's ability to respond and impact internal variability can result in complicated feedbacks where the controller can amplify or attenuate the frequency of internal variability, a feature explored thoroughly in MacMartin et al. (2014). These features of a controller are considered and balanced during the tuning phase of a controller. While this may present a challenge toawrds implementing a control algorithm in reality, Kravitz et al. (2014) showed that a control algorithm designed in one model could be used to meet the targets in a different model, demonstrating the controller's ability to generalize to different systems. The results in this work show a way to quantify a controller's sensitivities to a variety of temperature patterns post tuning, including to those outside of the system the control algorithm was tuned to. While the method produces some climate states that may have statistically low chances of occurring or that may never occur, it allows for quick and cheap quantification of internal variability's impact on the total injection determined by the controller. Results in this work are confined to the 2035 and 2045 base states calculated from the ARISE-SAI control simulations (i.e. temperature patterns are from the system the controller was tuned for). Given that this work shows that the internal variability's impact on the total injection depends on the background warming, using a different emissions scenario or model for the base state may result in different quantified sensitivities.

Once sensitivities are quantified, one can consider whether the magnitude in which different internal variability patterns impact the total injection is acceptable. For example, consider the ARISE-SAI controller's response to a Pinatubo-like eruption. It is straightforward that the controller injects less when there are naturally occurring aerosols cooling the planet. However, in regards to patterns of internal variability, is it acceptable that more SO_2 is injected when the atmospheric-ocean system is in an El Niño phase rather than a La Niña phase? Or should there be focus on ways to ensure that the majority of the SO_2 injection is in response to climate warming signal alone? Doing so would require the ability to separate the forced and unforced response in our current atmosphere or predict the future forced or unforced response with considerable accuracy. Given that knowing or predicting the forced or unforced response with high accuracy is an ongoing area of research (Dai et al., 2015; Mariotti et al., 2018; Xu & Darve, 2022), implementing current methods to determine the unforced and forced responses would introduce further uncertainty into the feedback system.

5 Conclusions

This work quantifies the ARISE-SAI controller sensitivity to internal variability and demonstrates a method that allows for a quick and effective quantification of controller sensitivity post tuning. The ARISE-SAI controller's response to patterns of internal variability associated with ENSO, NAO and SAM as well as a Pinatubo-like eruption are quantified as these patterns cover Northern Hemisphere, Southern Hemisphere, and global temperature impacts. Focus is placed on quantifying these patterns of internal variability in relation to years 2035 and 2045, which correspond to the deployment year in ARISE-SAI and the deployment year in delayed start, respectively (MacMartin et al., 2022). Using these two base state years, we show that internal variability's impact on the total injection is dependent on the background warming it is occurring un-

der. Using this method to explore and quantify sensitivities of a tuned controller provides the opportunity to explore controller responses to a system it is not tuned for, facilitates sensitivity comparisons between scenarios and earth system models, and may promote discussion about the extent to which an SAI-controller response to variability internal to the climate system.

Open Research Section

The CESM2-LE is available at the Climate Data Gateway https://climatedata.ibs.re.kr/data/cesm2-lens. The ARISE-SAI data is available at https://www.cesm.ucar.edu/community-projects/arise-sai. Code used in this work can be found at https://github.com/connollyc152/ExploreARISEcontroller and will be assigned a permanent doi on Zenodo upon publication. Processed data is available at https://datadryad.org/stash/share/xhAvfYZqNyA8d0w00pu03D_W9YJS_z6fCdjoM3poeLk and will be made available on Zenodo and given a doi upon publication.

References

Angell, J. K. (1990, July). Variation in global tropospheric temperature after adjustment for the el nino influence, 1958-89. *Geophys. Res. Lett.*, *17*(8), 1093–1096.

Åström, K. J., & Murray, R. M. (2021). *Feedback systems: an introduction for scientists and engineers.* Princeton university press.

Bluth, G. J., Doiron, S. D., Schnetzler, C. C., Krueger, A. J., & Walter, L. S. (1992). Global tracking of the so2 clouds from the june, 1991 mount pinatubo eruptions. *Geophysical Research Letters*, *19*(2), 151–154.

Cicerone, R. J. (2006, August). Geoengineering: Encouraging research and overseeing implementation. *Clim. Change*, *77*(3), 221–226.

Crutzen, P. J. (2006, August). Albedo enhancement by stratospheric sulfur injections: A contribution to resolve a policy dilemma? *Clim. Change*, *77*(3-4), 211–220.

Dai, A., Fyfe, J. C., Xie, S.-P., & Dai, X. (2015, April). Decadal modulation of global surface temperature by internal climate variability. *Nat. Clim. Chang.*, *5*(6), 555–559.

Deser, C., Phillips, A., Bourdette, V., & Teng, H. (2012, February). Uncertainty in climate change projections: the role of internal variability. *Clim. Dyn.*, *38*(3), 527–546.

Ho, M., Kiem, A., & Verdon-Kidd, D. (2012, March). The southern annular mode: a comparison of indices. *Hydrol. Earth Syst. Sci.*, *16*(3), 967–982.

Holasek, R., Self, S., & Woods, A. (1996). Satellite observations and interpretation of the 1991 mount pinatubo eruption plumes. *Journal of Geophysical Research: Solid Earth*, *101*(B12), 27635–27655.

Hurrell, J. W., & Deser, C. (2010, February). North atlantic climate variability: The role of the north atlantic oscillation. *J. Mar. Syst.*, *79*(3), 231–244.

Jarvis, A., & Leedal, D. (2012, July). The geoengineering model intercomparison project (GeoMIP): a control perspective. *Atmos. Sci. Lett.*, *13*(3), 157–163.

Kravitz, B., Caldeira, K., Boucher, O., Robock, A., Rasch, P. J., Alterskjaer, K., . . . Yoon, J.-H. (2013, August). Climate model response from the geoengineering model intercomparison project (GeoMIP). , *118*(15), 8320–8332.

Kravitz, B., MacMartin, D. G., Leedal, D. T., Rasch, P. J., & Jarvis, A. J. (2014, April). Explicit feedback and the management of uncertainty in meeting cli-

mate objectives with solar geoengineering. *Environ. Res. Lett.*, *9*(4), 044006.

Kravitz, B., MacMartin, D. G., Mills, M. J., Richter, J. H., Tilmes, S., Lamarque, J.-F., . . . Vitt, F. (2017). First simulations of designing stratospheric sulfate aerosol geoengineering to meet multiple simultaneous climate objectives. *Journal of Geophysical Research: Atmospheres*, *122*(23), 12–616.

Kravitz, B., Robock, A., Tilmes, S., Boucher, O., English, J. M., Irvine, P. J., . . . Watanabe, S. (2015, October). The geoengineering model intercomparison project phase 6 (GeoMIP6): simulation design and preliminary results. *Geosci. Model Dev.*, *8*(10), 3379–3392.

Liu, P. R., & Raftery, A. E. (2021, February). Country-based rate of emissions reductions should increase by 80% beyond nationally determined contributions to meet the 2 °c target. , *2*.

MacMartin, D. G., Kravitz, B., Keith, D. W., & Jarvis, A. (2014, July). Dynamics of the coupled human–climate system resulting from closed-loop control of solar geoengineering. *Clim. Dyn.*, *43*(1), 243–258.

MacMartin, D. G., Visioni, D., Kravitz, B., Richter, J. H., Felgenhauer, T., Lee, W. R., . . . Sugiyama, M. (2022, August). Scenarios for modeling solar radiation modification. *Proc. Natl. Acad. Sci. U. S. A.*, *119*(33), e2202230119.

Mariotti, A., Ruti, P. M., & Rixen, M. (2018, March). Progress in subseasonal to seasonal prediction through a joint weather and climate community effort. *npj Climate and Atmospheric Science*, *1*(1), 1–4.

National Academies of Sciences, Engineering, and Medicine. (2021). *Reflecting sunlight: Recommendations for solar geoengineering research and research governance.* National Academies Press.

Parker, D. E., Wilson, H., & Jones, P. D. (1996). The impact of mount pinatubo on world-wide temperatures. *J. Appl. Meteorol. Climatol.*.

Raftery, A. E., Zimmer, A., Frierson, D. M. W., Startz, R., & Liu, P. (2017, July). Less than 2 °c warming by 2100 unlikely. *Nat. Clim. Chang.*, *7*, 637–641.

Rasch, P. J., Crutzen, P. J., & Coleman, D. B. (2008). Exploring the geoengineering of climate using stratospheric sulfate aerosols: The role of particle size. *Geophysical Research Letters*, *35*(2).

Richter, J. H., Visioni, D., MacMartin, D. G., Bailey, D. A., Rosenbloom, N., Dobbins, B., . . . Lamarque, J.-F. (2022, November). Assessing responses and impacts of solar climate intervention on the earth system with stratospheric aerosol injection (ARISE-SAI): protocol and initial results from the first simulations. *Geosci. Model Dev.*, *15*(22), 8221–8243.

Rodgers, K. B., Lee, S.-S., Rosenbloom, N., Timmermann, A., Danabasoglu, G., Deser, C., . . . Yeager, S. G. (2021, December). Ubiquity of human-induced changes in climate variability. *Earth Syst. Dyn.*, *12*(4), 1393–1411.

Tilmes, S., Richter, J. H., Kravitz, B., MacMartin, D. G., Mills, M. J., Simpson, I. R., . . . Ghosh, S. (2018, November). CESM1(WACCM) stratospheric aerosol geoengineering large ensemble project. *Bull. Am. Meteorol. Soc.*, *99*(11), 2361–2371.

Tilmes, S., Richter, J. H., Mills, M. J., Kravitz, B., MacMartin, D. G., Vitt, F., . . . Lamarque, J.-F. (2017, December). Sensitivity of aerosol distribution and climate response to stratospheric SO 2 injection locations. *J. Geophys. Res.*, *122*(23), 12,591–12,615.

Trenberth, K. E. (1997, December). The definition of el niño. *Bull. Am. Meteorol. Soc.*, *78*(12), 2771–2778.

Wilson, J., Jonsson, H., Brock, C., Toohey, D., Avallone, L., Baumgardner, D., . . . others (1993). In situ observations of aerosol and chlorine monoxide after the 1991 eruption of mount pinatubo: effect of reactions on sulfate aerosol. *Science*, *261*(5125), 1140–1143.

Xu, K., & Darve, E. (2022, March). Physics constrained learning for data-driven inverse modeling from sparse observations. *J. Comput. Phys.*, *453*, 110938.